

Received July 28, 2018, accepted September 1, 2018, date of publication September 13, 2018, date of current version October 8, 2018.

Digital Object Identifier 10.1109/ACCESS.2018.2869943

Optimizing the Detection of Characteristic Waves in ECG Based on Processing Methods Combinations

KRESIMIR FRIGANOVIC¹, DAVOR KUKOLJA², ALAN JOVIC^{ID 1}, (Member, IEEE),
MARIO CIFREK^{ID 1}, (Senior Member, IEEE), AND GORAN KRSTACIC³

¹University of Zagreb Faculty of Electrical Engineering and Computing, 10000 Zagreb, Croatia

²Ericsson Nikola Tesla d.d., 10000 Zagreb, Croatia

³Josip Juraj Strossmayer University of Osijek, Faculty of Medicine, 31000 Osijek, Croatia

Corresponding author: Alan Jovic (alan.jovic@fer.hr)

This work was supported by the Croatian Science Foundation under Project UIP-2014-09-6889.

ABSTRACT Accurate detection of characteristic electrocardiogram (ECG) waves is necessary for ECG analysis and interpretation. In this paper, we distinguish four processing steps of detection algorithms: noise and artifacts reduction, transformations, fiducial marks selection of wave candidates, and decision rule. Processing steps combinations from several detection algorithms are used to find QRS, P, and T wave peaks. In addition, we consider the search window parameter modification based on waveform templates extracted by heart cycles clustering. The methods are extensively evaluated on two public ECG databases containing QRS, P, and T wave peaks annotations. We found that the combination of morphological mathematical filtering with Elgendi's algorithm works best for QRS detection on MIT-BIH Arrhythmia Database (detection error rate (DER) = 0.48%, Lead I). The combination of modified Martinez's PT and wavelet transform (WT) methods gave the best results for P wave peaks detection on both databases, when both leads are considered (MIT-BIH arrhythmia database: DER = 32.13%, Lead I, DER = 42.52%, Lead II; QT Database: DER = 21.23%, Lead I, DER = 26.80%, Lead II). Waveform templates in combination with Martinez's WT obtained the best results for T wave peaks detection on QT database (DER = 25.15%, Lead II). This paper demonstrates that combining some of the best proposed methods in literature leads to improvements over the original methods for ECG waves detection while maintaining satisfactory computation times.

INDEX TERMS ECG, characteristic waves, automatic detection algorithms, clustering, expert system, biomedical signal analysis.

I. INTRODUCTION

Electrocardiography has been used as a heart diseases' diagnostic tool for many years. Electrocardiogram (ECG) reflects electric polarization and depolarization of the heart chambers. Characteristic waves in ECG are known as P wave, QRS complex, and T wave. P wave reflects depolarization of the atria, QRS complex corresponds to ventricular depolarization, and T wave represents ventricular repolarization, i.e. restoration of the resting membrane potential [1]. The repolarization of atria is concealed by depolarization of ventricles.

Cardiologists monitor patients' health visually, by inspecting signal morphology present in ECG record (usually all 12 leads of standard ECG). This requires a tremendous amount of time and expert human resources with specialized education and practice. To deduct the time and amount of

required doctors' attention per patient, a computer based expert system for processing and analysis of ECG records and diagnosis of the cardiovascular diseases can be of great help.

Duration and amplitude of ECG waves (P, QRS, T) and segments between the waves (ST segment, QT interval, PR interval) are used to indicate and detect patients' normal or abnormal heart rhythm and state of health. Additional diagnostic characteristics related to ECG morphology include: P wave absence and presence of fibrillatory waves in atrial fibrillation; J point amplitude (from baseline), R/S wave ratio, ST segment slope in acute myocardial ischemia, etc. [2]. Heart rate variability, a time series extracted from cardiac interbeat (R-R) intervals, is also an important indicator of patient's overall health and may be used to help detect particular disorders, such as congestive heart failure [3].

Precise detection of R waves is an essential step in deriving the heart rate variability time series.

Accurate detection of amplitude and time index of peaks, onset and offset points of all characteristic ECG waves is required to extract features for development of an expert system for heart condition diagnoses, ECG recognition and other applications [4]. In this respect, detection of QRS complex (especially, the R spike peak) is a highly researched topic, due to attainability of annotated signal databases. Accuracy in the sense of sensitivity and positive predictive value is above 99% in most of the related works [5]–[10]. On the other hand, detection of P and T waves is still unsatisfactory, due to limited availability of annotated datasets [11]. Different approaches have been researched in order to analyze characteristic waves in ECG signals: algorithms based on various derivates and threshold decisions, algorithms based on complex transformations, such as wavelet [12]–[15] and Hilbert-Huang transforms [16]–[20], or algorithms that use machine learning methods, like artificial neural networks [21], [22].

The majority of proposed algorithms in literature are evaluated on a single major lead (mostly MLII), as it yields the best representation of ECG characteristic waves. The reported accuracy evaluation in literature lacks the information on how well the algorithms perform on other leads, as they may be accidentally switched during recording sessions. Also, the evaluation of the algorithms' results depends on the exact determination of the ECG characteristic wave points, which is performed by comparing with the already given annotations. This process does not allow compare the results of the algorithms' individual processing steps. In this work, we divided algorithms into processing steps to evaluate improvements in detection accuracy of characteristic ECG waves, when specific steps are combined.

We concentrate on five algorithms which are numerically efficient and do not require training sets. From these algorithms, we distinguish four processing steps in ECG characteristic wave detection, namely: 1) noise and artifact reduction, 2) transforms, 3) fiducial marks selection of wave candidates, and 4) decision rule (similar to three steps reported in [5]). Based on these steps, we aim at adapting the described detection algorithms by combining certain steps for the optimal waves' detection capabilities. Moreover, we explore the search window parameter modification based on template waveforms extracted by heart cycles clustering. This work is the continuation of our previous study that aimed at maximal accuracy of ECG waves detection [23]. Our primary motivation is to provide an efficient online service to both medical professionals and engineers, related to the analysis of multiple heterogeneous biomedical time series [24].

The contributions of this work are, as follows.

- 1) We show that algorithms' accuracy can be improved both for QRS complex and P and T waves peaks detection, which is achieved by considering combinations of the processing steps and methods.

- 2) We introduce parameter modification based on waveform templates extracted by heart cycles clustering and show that particular methods for P and T waves peaks detection may benefit from this method.
- 3) We present a modification of Martinez's algorithm based on phasor transform (PT).

The paper is structured as follows. Section II describes the algorithms and their combinations, parameter modification based on template waveforms, and the used databases. Section III summarizes the results obtained for the different analyzed databases. The outcomes are discussed in section IV. Finally, section V presents the concluding remarks and intended future work.

II. METHODS

A. ALGORITHMS' OVERVIEW

Five ECG characteristic waves' detection algorithms are considered in this paper. The purpose of this subsection is to provide a brief and concise description of the algorithms. As one of the algorithms also required some modifications, the modifications are also explained in detail here. For the more in-depth descriptions of the non-modified algorithms, we refer the reader to the given references.

The reported detection results in terms of sensitivity (Se) and positive prediction (PPV) of the algorithms considered in our work are given in Table 1. The algorithms are selected based on their different approaches to processing steps (like Pan Tompkins' adaptive thresholding, mathematical morphological transform from Sun *et al.*, phasor and wavelet transforms from Martinez and moving average approach from Elgendi). A comparative study of ECG segmentation algorithms (which includes three of the algorithms considered in this paper) can be found in [25]. We note that there are other algorithms found in literature that use similar processing steps and match our selection rule (numerically efficient and do not require training sets), such as Vázquez-Seisdedos *et al.* [26], with the proposed geometric method, Vítek *et al.* [27], with the continuous wavelet transform, Singh and Gupta [28], with the maximum vertical offset, Di Marco and Chiari [29], with the discrete wavelet transform and adaptive thresholding. However, in this paper, we consider only the five algorithms that reported the best accuracy in detection of the wave peaks.

1) PAN TOMPKINS

Pan Tompkins is a well known algorithm for R spike detection, described in [5]. The first step of this algorithm is to filter signal with a desirable bandpass filter to maximize the QRS energy. The frequency band chosen in the original paper is 5–15 Hz. The band is realized with a cascade of low and high-pass filters. In the original paper, the filters were designed for the sampling frequency of 200 Hz. To provide the QRS complex slope information, the filtered signal is differentiated, squared and integrated with a moving average window of 150 ms width in order to make all data positive and to obtain relevant waveform feature information.

TABLE 1. Results of detection accuracy reported by researchers.

Algorithm	P peak detection accuracy	QRS detection accuracy	T peak detection accuracy
Pan Tompkins [5]	/	Se = 99.76% PPV = 99.56%	/
Elgendi et al. [6][30]	Se = 98.05% PPV = 97.11%	Se = 99.78% PPV = 99.87%	Se = 99.86% PPV = 99.65%
Martinez et al. (WT) [31]	Se = 98.87% PPV = 91.17%	Se = 99.80% PPV = 99.86%	Se = 99.77% PPV = 97.79%
Sun et al. [32]	Se = 97.2% (P onset)	Se = 100% (QRS onset)	Se = 99.80% (T onset)
Martinez et al. (PT) [33]	Se = 98.65% PPV = 97.52%	Se = 99.71% PPV = 99.97%	Se = 99.20% PPV = 99.01%

Fiducial marks are extracted from the peaks or maximum slopes of the signal, after which the unique adaptive threshold decision making on the QRS candidates is applied. Pan Tompkins' algorithm is a very simple, yet effective, algorithm for QRS complex detection.

2) ELGENDI's ALGORITHM BASED ON TWO MOVING AVERAGE FILTERS

Elgendi's algorithm is a somewhat novel algorithm for QRS detection described in 2013 [6]. Similar to Pan Tompkins' algorithm, the first step is a Butterworth passband filter. Thereafter, the squaring is applied. To extract the fiducial marks (or blocks of signals which are containing fiducial marks, called blocks of interest), two moving averages are applied. The width of both moving average (MA) windows are based on *a priori* knowledge about the average ECG intervals, chosen to fit the width of QRS complex (for the first moving average filter), and the width (duration) of one heartbeat (for the second moving average filter).

Blocks of interest are segments of signal where the output from the first moving average filter (MA1) exceed the output from the second one (MA2), with the addition of a threshold offset. If the block width is greater than or equal to the width of the first MA window, it is classified as QRS complex. The absolute maximum value in a block is classified as an R spike. Elgendi found that the optimal algorithm parameters (tested on the MIT-BIH Arrhythmia Database) are: passband filter frequency band set to 8-20 Hz, window width for the first MA (W1) equal to 97.2 ms and for the second MA (W2) equal to 611 ms.

Elgendi et al. [30] adapted the described algorithm for the detection of P and T peaks with the width of W1 and W2 equal to half of the average P wave duration (55 ms) and average T wave duration (110 ms), respectively. Blocks of interest are searched in respect to R peaks.

3) SUN YAN's ALGORITHMS BASED ON MATHEMATICAL MORPHOLOGY OPERATIONS

Sun Yan's algorithm for characteristic ECG waves detection is described in [32]. It uses multiscale morphological derivative (MMD) with fixed scale to enhance the slopes in signal. Preprocessing is done with mathematical morphological

filtering (MMF) for noise reduction and baseline correction, which is described in [34]. Local minima are considered as the fiducial marks for R waves, as the slope of the QRS complex produces negative local minimum after the MMD transformation. Thresholding decision is set by the histogram of the MMD transformed data. Unfortunately, the histogram method is not adequately described in the paper, so we did not implement it in our work. After detecting the R wave, simple peak search loop is applied in order to determine the peaks, offsets and onsets of P and T waves.

4) MARTINEZ'S ALGORITHMS BASED ON WAVELET TRANSFORM

Martinez et al. [31] developed an algorithm for ECG wave delineation based on wavelet transformation (WT) approach adapted from [35]. The algorithm applies WT with a quadratic spline [36] for prototype wavelet $\psi(t)$ over the digitized ECG signal without any prefiltering. Using the *algorithme à trous* filter-bank implementation of WT, the frequency responses of the first five scales ($2^1 - 2^5$) are computed.

For QRS detections, the algorithm searches across the scales for "maximum modulus lines" exceeding adaptive thresholds at scales 2^1 to 2^4 . The zero crossing of the WT at scale 2^1 between a positive maximum - negative minimum pair, or negative minimum - positive maximum (for negative waves) is then marked as a QRS.

For T wave detection, the algorithm looks for local maxima of WT at scale 2^4 in the search window defined with the QRS position and RR interval. T wave is present if at least two local maxima exceed the threshold ϵ_T . In that case, the local maxima of WT greater than γ_T are considered as slopes of the wave and the zero crossing between them as the wave peak. The strategy to identify the P wave peak is similar, except the thresholds ϵ_P and γ_P are adjusted for P peak detection.

5) MARTINEZ'S ALGORITHM BASED ON PHASOR TRANSFORM WITH MODIFICATIONS

Martinez et al. [33] describes a novel ECG delineator based on phasor transform (PT). PT converts each ECG sample into a complex number (called phasor), preserving its information regarding magnitude and phase values. With the application of PT to the ECG signal, the slight wave variations in the original signal are maximized.

According to [33], the PT algorithm for QRS detection has a sensitivity of 99.71% and a positive predictive value of 99.97% on MIT-BIH Arrhythmia Database. With all our efforts in changing the baseline removal filter and the normalization method, we have never got the results in the same range. Therefore, we have used Martinez's PT algorithm only for P and T wave detection, with R peaks vector as an input parameter. For the input R peaks vector, depending on the application, referent record's R peaks annotations or R peaks detected with some other QRS detection method were used.

During the implementation of the Martinez's PT algorithm, we had to introduce some modifications, because the authors

did not fully explain all steps, especially the necessary preprocessing operations before applying the PT, a fact also noted in [37]. In continuation, wherever we mention Martinez's PT algorithm, we imply our modified version.

The first step of our modified algorithm was forward/backward filtering using third order Butterworth passband filter with frequency band 0.5-20 Hz in order to remove baseline wander and high frequency noise from ECG signal, as a combination of original Martinez's and Elgendi's algorithm preprocessing step. ECG normalization to range $[-1 \ 1]$ was implemented by dividing the whole ECG signal with its maximum R-peak amplitude after discarding outliers spikes, which was implemented by discarding 0.1% of the largest ECG signal samples.

For identification of Q and S waves, the modified algorithm starts from the input R peaks vector. The algorithm first detects two boundary points, γ_{QRS-} and γ_{QRS+} as the closest points to the R peak in which the phase variation is lower than $\pi/8$. We have also included a time constraint: an interval between γ and R peak cannot be longer than 0.1 s. Otherwise, the threshold, initially set to $\pi/8$, is increased by 0.05 rad and the process of γ point detection is repeated until the time constraint is satisfied. The algorithm then creates a window of 55 ms before the boundary point γ_{QRS-} in order to search for the Q wave. For the defined window, increased when compared to the original algorithm, the algorithm applies PT to the absolute value of the ECG, subtracting previously the median of the segment.

According to the original algorithm, if, in the search window, no point presents a phase higher than 50% of the maximum variation within the window, the local minimum is annotated as a Q point. Otherwise, the point with the highest magnitude among those exceeding threshold is annotated as a Q point. In our modification, we have used a constraint for which the Q wave is located in the interval between γ_{QRS-} and a positive peak closest to the R peak. If there are no positive peaks, the point where the elbow in the ECG signal is the largest is annotated as the Q point. Similar strategy is used for S wave delineation. The only difference is that the search window is placed after the γ_{QRS+} point.

For P and T waves peak detection, the PT algorithm is modified in a way that introduces a sliding search window across search segment with fixed boundaries. For P wave search, the segment is defined as the initial search window in the original Martinez's PT algorithm, the length of the search window is a quarter of the last RR interval with the Q peak position as a boundary. Initially, the length of the search window is the same as the search segment and, if no P peak is detected, the width of the search window is iteratively reduced until the detection of the P wave peak using the original PT detection method is obtained [27]. For T wave detection, the length of the search segment is doubled to a half of the last RR interval and the S wave is considered as the boundary point. Furthermore, because the original PT algorithm presumes that the T wave is always positive,

and cannot detect inverted T waves, we have modified the rule for T peak detection. The local phase maximum is annotated as a T peak if the point is the peak and if its magnitude is 3 times larger than the magnitude of the local minimum. The local phase minimum is annotated as a T peak if the point is the peak and if its magnitude is 2.7 times larger than the magnitude of the local maximum.

We summarize the list of modifications made to the Martinez's PT algorithm below:

- 1) Forward/backward filtering using third order Butterworth passband filter with frequency band 0.5-20 Hz
- 2) ECG normalization after discarding outliers spikes (discarding 0.1% of the largest ECG signal samples)
- 3) A time constraint for an interval between γ and R peak interval
- 4) Increased Q wave window search
- 5) A constraint for which the Q wave is located in the interval between γ_{QRS-} and a positive peak closest to the R peak, similarly for the S wave
- 6) The point where the elbow in the ECG signal is the largest is annotated as the Q point
- 7) Introduction of a sliding search window across for P and T wave peak detection
- 8) Modified T wave peak detection rule

In this work, we also try the combination of Martinez's WT and Martinez's PT algorithm. In this combination, we used QRS onset and QRS offset obtained by Martinez's WT algorithm as an input to determine the boundaries for search segments during the detection of P and T waves with the modified Martinez's PT algorithm.

B. DATA

Two databases are used in this work to evaluate the methods: MIT-BIH Arrhythmia Database [38] and QT database [39], both freely available from the PhysioNet portal [40]. The databases were chosen based on the availability of both QRS and P and T wave annotations. A brief description of the used databases are given in this subsection.

1) MIT-BIH ARRHYTHMIA DATABASE

The database contains 48 ECG recordings sampled at 360 Hz. The duration of each recording is 30 minutes. Recordings 102, 104, 107, and 217 were excluded from the analysis because of the paced beats presence. Recording 207 was also excluded due to a great number of ventricular flutter waves. MIT-BIH Arrhythmia Database is widely used for testing the R peak detection algorithms. Accessibility of P and T wave annotations were limited to the QT database for public use. Elgendi *et al.* [41] generously made a publicly available reannotation of MIT-BIH Arrhythmia Database that now includes P and T waves annotations. Due to attainability of only peak annotations for MIT-BIH Arrhythmia Database, detection of onsets and offsets of each wave (QRS complex, P and T wave) are not considered in the current paper.

TABLE 2. The number of analyzed recordings and annotated waves peaks in the selected databases.

Database	No. of records	No. of leads	Sampling rate	R peaks annots	P peaks annots	T peaks annots
MIT-BIH Arrhythmia Database	43	2	360	98873	95989	98395
QT database	105	2	250	86357	3194	3542

2) QT DATABASE

The database contains 105 ECG records, which are sampled at (or resampled to) 250 Hz. The duration of each recording is 15 minutes. Only the last 5 minutes of the records are annotated. The records in QT Database were taken from seven different databases. A section of ECG record is selected in order to avoid significant baseline wander or other artifacts. Between 30 and 100 representative beats were manually annotated by cardiologists in each record, who identified the onset, peak, and offset of P waves, onset, peak, and offset of QRS complexes, the peak and offset of T waves, and (if present) the peak and offset of U-waves [39]. Annotations in *.atr* format, reference beat annotations from the original database, were recalculated for record *sel232* in the QT database on the basis of the record 232 annotations from the MIT-BIH Arrhythmia Database. We tested the algorithms on the whole dataset, wherever the annotations were available. We used only *.atr* annotations of R peaks and compared only P and T waves peaks that are annotated.

The characteristics of the used records from both databases are given in Table 2. The algorithms were tested on both available leads for each record. For the record *114* in MIT-BIH Arrhythmia Database (and *sel114* of the QT database) the leads were switched, as recommended in [38].

C. EXPLORATION OF PROCESSING STEPS COMBINATIONS

Each of the algorithms described in Section II.A. can be separated into four processing steps:

- 1) noise and artifact reduction (preprocessing)
- 2) transformations that enhance the desired property of the wave (e.g. slope of the QRS complex)
- 3) fiducial marks selection
- 4) decision if the selected fiducial marks represent characteristic wave peak.

In this subsection, we elaborate on the procedure for combining various processing steps.

We explored the influence of the selected preprocessing step on the algorithms, so we combined the preprocessing step of Elgendi's and Sun Yan's algorithms (MMF) with the other algorithms to improve noise and artifact reduction. Also, MMD transformation step was introduced into the combinations to test its behavior within Elgendi's and Martinez's WT and PT algorithms. Adaptive thresholding from Pan Tompkins' algorithm was combined with

Elgendi's algorithm, to explore possible improvements in the reduction of false positives detection.

Fig. 1 shows the decomposition of the described algorithms into four processing steps for R peak detection. We do not delve into the mathematical details of the specific steps for the inspected algorithms, as these are given in the corresponding literature. In the upper block diagram of Fig. 1, the steps of QRS detection algorithms are shown. Below that, a block diagram describing the combinations of the processing steps is shown. In the given example, MMF and MMD are added to Elgendi's algorithm as an additional preprocessing step. In Fig. 2, the P and T waves detection processing steps are presented, along with an additional combination block diagram. Dashed lines in the block diagrams in Fig. 1 and Fig. 2 indicate signal paths from the original algorithms.

As the number of all possible combinations is quite large, not all combinations are presented in the Results section. The combinations which yielded poor results (such as the combinations of MMF, MMD and Martinez's PT algorithm) are not presented or discussed. Here follows the list of methods that we evaluated, and later compared, with the results of the original algorithms (section IV).

QRS complex detection:

- Method 1: Pan Tompkins' original algorithm (5 – 15 bandpass filtering)
- Method 2: Pan Tompkins' algorithm with 8 – 20 bandpass filtering
- Method 3: mathematical morphological filtering (MMF) with Pan Tompkins' algorithm
- Method 4: Elgendi's algorithm
- Method 5: mathematical morphological filtering (MMF) with Elgendi's algorithm
- Method 6: multiscale morphological derivative (MMD) with Elgendi's algorithm
- Method 7: MMF with MMD and Elgendi's algorithm
- Method 8: Elgendi's algorithm with Pan Tompkins' adaptive thresholding
- Method 9: Martinez's WT algorithm
- Method 10: mathematical morphological filtering (MMF) with Martinez's WT algorithm
- Method 11: multiscale morphological derivative (MMD) with Martinez's WT algorithm
- Method 12: MMF with MMD and Martinez's WT algorithm

P and T wave detection:

- Method 1: Martinez's PT algorithm
- Method 2: Martinez's PT algorithm with templates (described in Section II.D)
- Method 3: Martinez's WT algorithm
- Method 4: Martinez's WT algorithm with templates (described in Section II.D)
- Method 5: Martinez's WT with Martinez's PT algorithms
- Method 6: Elgendi's algorithm

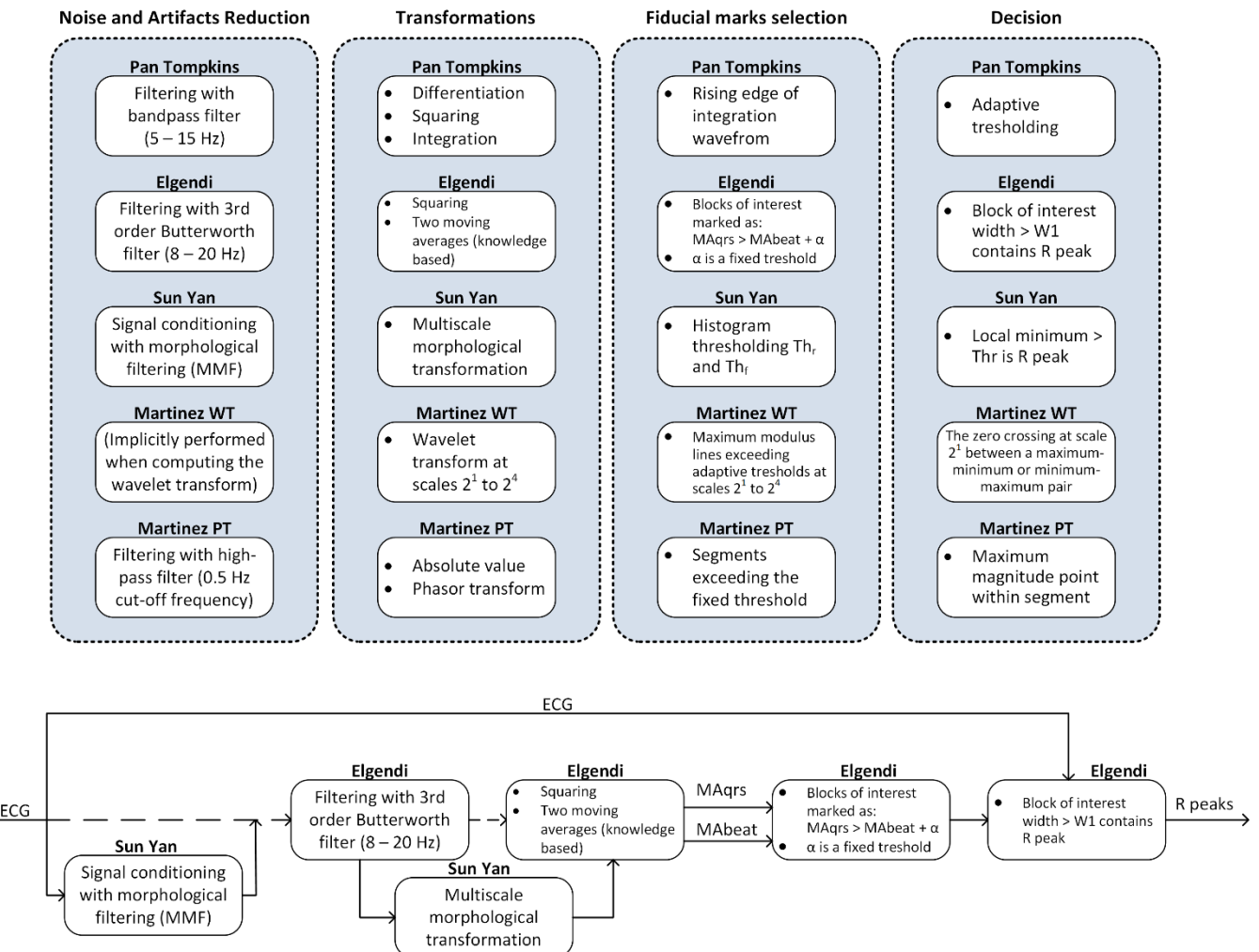


FIGURE 1. Processing steps in the detection algorithms of ECG R peaks (above) and block diagram example of processing step combination for R peak detection (below, the example of QRS complex detection method 7 – combination of MMF with MMD and Elgendi’s QRS detection algorithm).

- Method 7: mathematical morphological filtering (MMF) with Elgendi’s algorithm
- Method 8: mathematical morphological filtering (MMF) with Martinez’s PT algorithm
- Method 9: MMF with Martinez’s WT algorithm
- Method 10: MMF with MMD and Martinez’s WT algorithm

D. SEARCH WINDOW PARAMETER MODIFICATION BASED ON WAVEFORM TEMPLATES EXTRACTED BY HEART CYCLES CLUSTERING

During the fiducial mark selection step for the detection of P and T waves, search windows are set relative to R peaks. The parameters of the search windows are based and defined according to the standard waveform in RR interval. This causes problems in detection when there is a large deviation from this standard. To address this problem, we explore the search window parameter modification based on waveform templates. Here, we describe the novel approach of using waveform templates to improve the detection of P and T wave peaks.

Parameter modification based on waveform templates is inspired by [42], where heart cycles are clustered based on features calculated from time duration and geometry of the cycles. We have opted for the approach to cluster heart cycles by the shape of the time series using the k -spectral centroid algorithm [43], a time series clustering algorithm which uses a similarity metric that is invariant to scaling and shifting. This method finds the most representative shape (the cluster centroid) for each cluster. This is important for our application, because the most representative shapes are in fact the most representative heart cycle waveform templates. By using the k -spectral centroid algorithm, instead of some clustering method based on features calculated from time series, the influence of features to the shape of the obtained template is avoided, as the clusters deal with the time series directly.

According to [42], the complete heart cycle is defined physiologically as the ECG segment which begins at the P wave onset and ends with the T wave offset. However, because the first step of ECG delineation is QRS complex detection, the sequence of heart cycles is assumed to

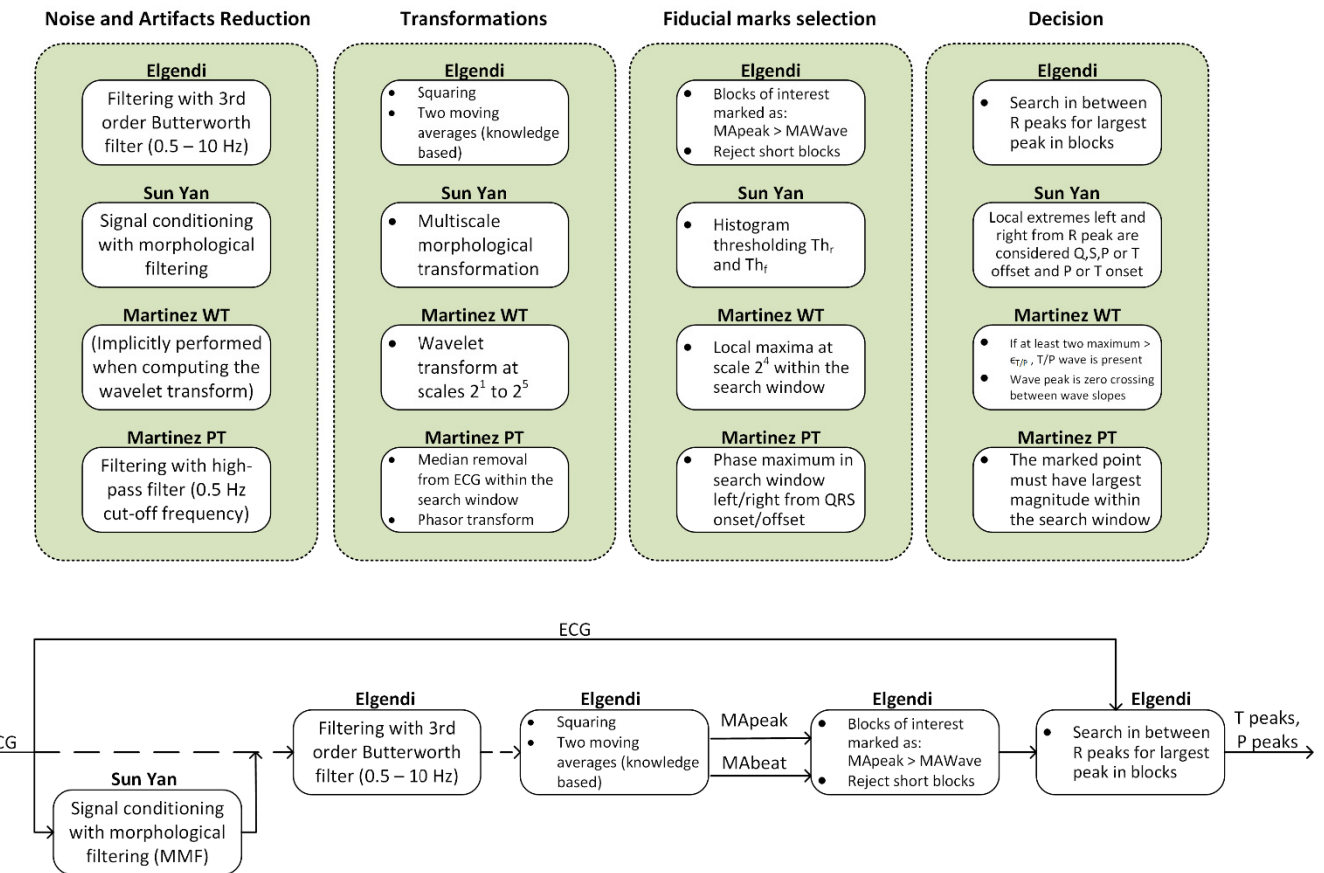


FIGURE 2. Processing steps in the detection algorithms of ECG P and T waves (above) and a block diagram example of processing step combination for P and T peaks detection (below, the example of P and T peaks detection method 7 – the combination of MMF and Elgendi's P and T wave peaks detection algorithm).

be RS-T-P-QR, instead of P-QRS-T. Using this assumption, the complete heart cycle can be defined as RR interval time series – the ECG segment located between two successive R waves.

In this study, the performance of the algorithm for waveform templates extraction is verified on the MIT-BIH Arrhythmia Database (without records 102, 104, 107, 207 and 217). For all selected records, we have used the MLII lead.

To get the most representative clusters, in the first step, we filtered all the records using third order Butterworth passband filter with frequency band 0.5-20 Hz to remove baseline wander and high frequency noise from ECG signal. Then, we normalized ECG signals to the range $[-1, 1]$ by dividing the whole ECG signal with its maximum R peak amplitude after discarding 0.1% of the largest ECG signal samples. The normalization was necessary in order to enable comparison of records from different databases, because ECG signals can be recorded with different amplifications. After the normalization, R peaks were automatically reannotated in a way that the closest local peaks were considered to be better R peak annotations for the selected lead. The reason for R peak reannotation was that the R peaks were annotated

using the multilead criteria, while during clustering, we use only a single lead.

Using the described process, we obtained 98 830 RR intervals. Because RR interval shape depends on the interval duration, we divided the obtained set into 5 subsets with an equal number of RR intervals. In the first subset, we have the shortest intervals, and, for all subsequent subsets, all intervals are longer than in the previous subset, ending with the longest intervals in the fifth subset.

To cluster the time series with the k -spectral centroid algorithm, all the time series must have an identical length. Furthermore, the identical length of the time series is also necessary for comparison of records with different sampling frequencies. Therefore, we have resampled every RR time series to 251 points using the piecewise cubic Hermite interpolation [44], [45]. The number of points was initially determined as one second (RR interval duration at 60 bpm), sampled at 250 Hz (QTDB sampling rate). Afterwards, it was experimentally determined that this is a sufficient number for waveform description because the shapes of all RR intervals remained the same after the resampling. We applied the piecewise cubic Hermite interpolation, because it preserves monotonicity and the shape of the data. Then, for all 5 subsets,

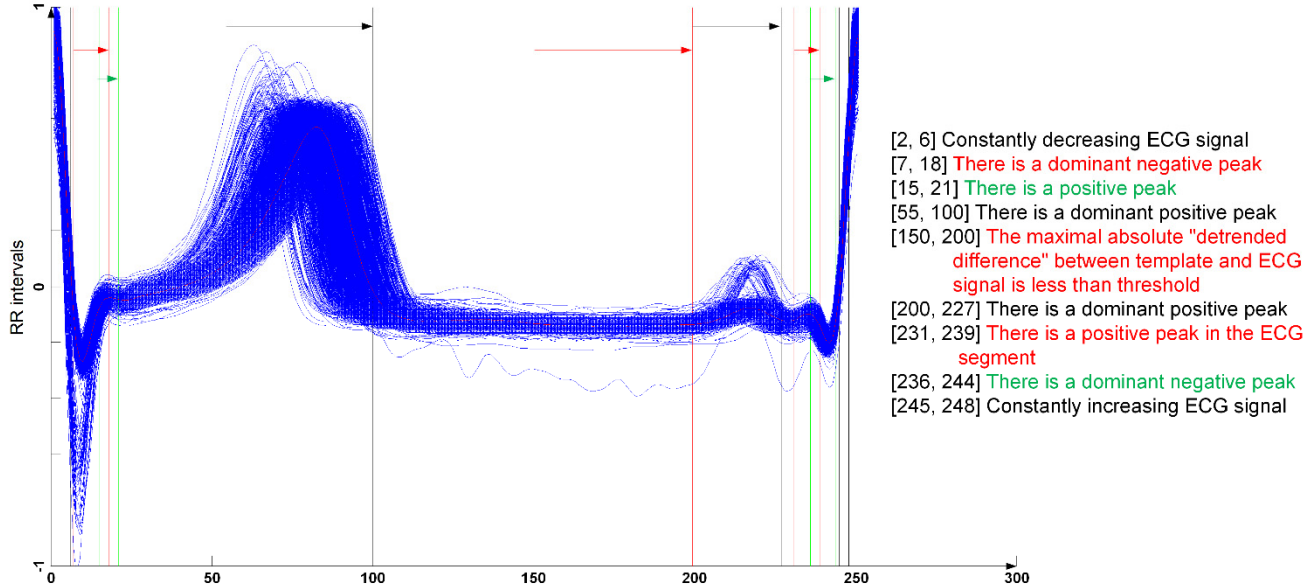


FIGURE 3. Example of membership rules assignment to a waveform template and RR intervals from the MIT-BIH Arrhythmia Database that satisfy them.

we clustered the RR interval time series based on their shape into 20 clusters with the k -spectral centroid algorithm. With the heart cycles clustering process, we created 100 representative waveform templates of RS-T-P-QR heart cycles. The number of subsets, and the number of clusters are determined using the elbow method.

To determine whether some RR interval belongs to the waveform template, we implemented the membership rules strategy. For each cluster, we manually, in collaboration with cardiologists, assigned a subset of rules that describe it, together with the waveform template. We implemented the following set of rules that can be assigned to each ECG segment of a waveform template:

- 1) There is a negative peak in the ECG segment.
- 2) There is a positive peak in the ECG segment.
- 3) There is no fluctuation in the ECG segment – there is no negative or positive peak with amplitude larger than 0.01.
- 4) There is a dominant negative peak in the ECG segment – there is a negative peak with amplitude larger than 60% of waveform template's amplitude. The absolute difference between the ECG value at the start of the segment and the local minimum, and the absolute difference between the local minimum and the ECG value at the end of the segment have to be at least 30% of those in the template. Furthermore, there is no positive peak with the amplitude larger than the amplitude of the negative peak.
- 5) There is a dominant positive peak in the ECG segment – there is a positive peak with an amplitude larger than 60% of waveform template's amplitude. The absolute difference between the ECG value at the start of the

segment and the local maximum, and the absolute difference between the local maximum and the ECG value at the end of the segment have to be at least 30% of the template's ones. Furthermore, there is no negative peak with the amplitude larger than the amplitude of the negative peak.

- 6) There is no negative peak in the ECG segment.
- 7) There is no positive peak in the ECG segment.
- 8) There is a constantly decreasing ECG signal in the defined interval.
- 9) There is a constantly increasing ECG signal in the defined interval.
- 10) The maximal absolute difference between the template and the ECG signal is less than 0.1 in the defined interval.
- 11) The maximal absolute "detrended difference" between the template and the ECG signal is less than 0.05 in the defined interval.
- 12) There is no dominant negative peak in the ECG segment – there is no negative peak with the amplitude larger than 0.1.
- 13) There is no dominant positive peak in the ECG segment – there is no positive peak with amplitude larger than 0.1.
- 14) The amplitude of the negative peak is larger than the amplitude of the positive peak in the ECG segment.
- 15) The amplitude of the positive peak is larger than the amplitude of the negative peak in the ECG segment.

Fig. 3 shows an example of membership rules assignment to a waveform template. In Fig. 3, we can observe the RR intervals plotted with blue lines, which satisfy all membership rules assigned to that waveform template, and

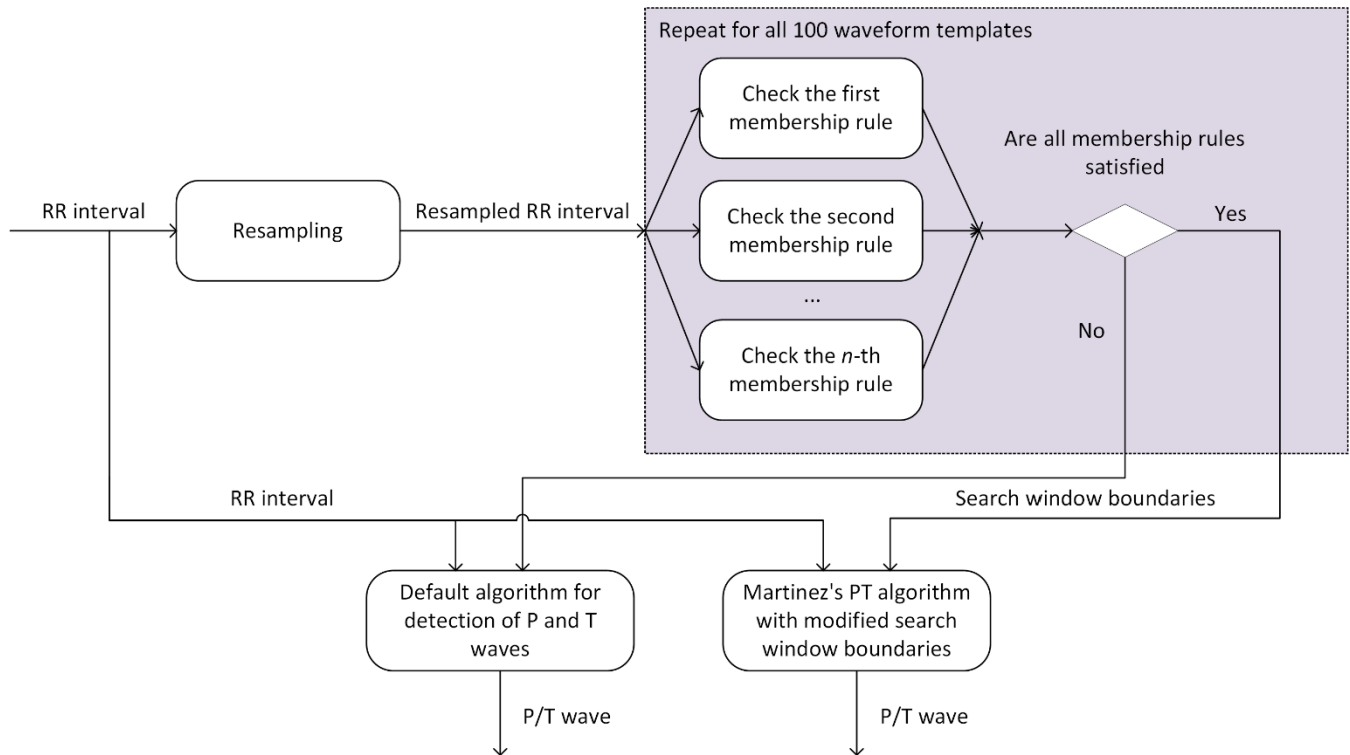


FIGURE 4. P and T wave detection strategy using the waveform templates.

the waveform template plotted with a red-black line. In this example, assigned membership rules are: the RR interval must be constantly decreasing in the sample interval [2, 6] (marked with a black arrow), there is a dominant negative peak in the sample interval [7, 18] (marked with a red arrow), there is a positive peak in sample interval [15, 21] (marked with a green arrow), etc. The list of rules is marked on the right side of Fig. 3.

The strategy for using waveform templates during P and T wave detection is illustrated in Fig. 4. For every RR interval in a record, the algorithm has determined whether it belongs to some waveform template: in the first step, an RR interval was resampled to 251 points using the piecewise cubic Hermite interpolation, and afterwards, for all 100 templates, the algorithm checked whether all the membership rules for each template are satisfied. If an RR interval did not belong to any of the templates, P and T waves were detected by the default detector. In the Martinez's PT + templates combination, the default detector is the Martinez's PT algorithm and, in the Martinez's WT + templates combination, the default detector is the Martinez's WT algorithm. Otherwise, P and T waves were detected with Martinez's PT algorithm with the modified parameters.

This procedure was possible to apply, because we have, in cooperation with the cardiologists, annotated the intervals where fiducial points are located in the ECG for each template. Except for the intervals, which served as modification for the P/T wave search window boundaries in Martinez's

PT algorithm, sometimes additional information about the template, like “no P/T wave is present in the template” or “wave is positive/negative/biphasic”, have also changed the P/T wave detection algorithm. For example, a waveform template illustrated in Fig. 3 has the following annotated intervals:

- 1) T wave is positive with peak located in sample interval [55, 100]
- 2) P wave is positive with peak located in sample interval [200, 227].

E. EVALUATION PROCEDURE

In order to calculate the performance of the detection algorithms, four parameters were calculated: sensitivity (Se), positive predictive value (PPV), detection error rate (DER) and F1 score (F1):

$$Se = \frac{TP}{TP + FN} \quad (1)$$

$$PPV = \frac{TP}{TP + FP} \quad (2)$$

$$DER = \frac{FP + FN}{TP + FN} \quad (3)$$

$$F1 = \frac{2TP}{2TP + FP + FN} \quad (4)$$

For determination of true positives (TP) in QRS complex peak detection, a sample deviation of 75 ms equivalent is used, based on AAMI ECAR recommendations [46].

TABLE 3. Average F1 score (%) and sum of DER (%) of both leads for every method and database.

Method	MIT-BIH R wave		QTDB R wave		Method	MIT-BIH P wave		MIT-BIH T wave		QTDB P wave		QTDB T wave	
	F1	DER	F1	DER		F1	DER	F1	DER	F1	DER	F1	DER
Pan Tompkins (5 - 15)	95.18	19.04	95.82	16.84	Martinez PT	80.06	76.12	67.08	128.36	87.58	49.84	83.32	66.35
Pan Tompkins (8 - 20)	97.04	11.79	97.28	10.92	Martinez PT + templates	/	/	/	/	87.40	50.31	84.28	62.51
MMF + Pan Tompkins	96.45	14.16	97.26	11.04	Martinez WT	72.13	104.61	64.45	139.11	85.49	58.14	87.69	49.18
Elgendi	97.86	8.54	96.61	13.73	Martinez WT + templates	/	/	/	/	86.77	52.50	88.00	48.00
MMF + Elgendi	97.29	10.83	97.42	10.40	Martinez WT + PT	80.73	74.65	65.63	136.21	88.28	48.03	84.85	60.90
MMD + Elgendi	97.06	11.72	88.33	47.24	Elgendi	58.24	169.07	70.24	115.54	69.52	129.62	76.76	93.17
MMF + MMD + Elgendi	97.27	10.89	93.52	26.08	MMF + Elgendi	49.57	204.57	71.86	110.84	44.17	237.88	78.05	88.54
Elgendi + Adaptive Thresh.	96.58	13.39	96.75	13.09	MMF + Martinez PT	77.39	84.89	61.87	150.03	81.00	74.23	85.24	59.26
Martinez WT	90.14	38.59	92.55	29.94	MMF + Martinez WT	69.59	112.96	61.81	147.52	76.36	90.20	85.44	57.65
MMF + Martinez WT	86.38	51.72	88.02	47.57	MMF + MMD + Martinez WT	56.87	157.80	51.64	180.93	71.30	113.21	71.69	110.47
MMD + Martinez WT	91.17	36.06	93.11	41.82									
MMD + MMF + Martinez WT	92.85	29.15	94.10	24.40									

Hence, if the detected peak is in the range of ± 75 ms from the annotated peak, the value is considered TP. Otherwise, it is considered false positive (FP). Similarly, if no detection of a peak was made in the range of ± 75 ms around the annotation, the detection was considered false negative (FN). The sample deviation of ± 75 ms is also used in the algorithms for the detection of P and T wave peaks. During the evaluation procedure, the detection of P and T wave peaks is independent of QRS complex peak detection. Whether or not the algorithm supports detection of QRS complexes, the detection of P and T wave peaks for evaluation purposes has always started from the annotated QRS complex peaks. In this way, the possible deterioration of the P and T wave peaks detection for algorithms that also support detection of QRS complex peak is eliminated.

To determine the computational cost of each method, we measured the time required for the methods to analyze 30-minute long ECG recordings from the MIT-BIH Arrhythmia Database. As each of the RR intervals is checked individually for the template membership, the template membership rule assignment computation time is measured for a single RR interval. Also, the computation times for different lengths of ECG records are explored. The algorithms were implemented and executed in Matlab R2017b on a computer with Windows 10 OS, Intel Core i7 CPU at 2.60 GHz and 8 GB of RAM memory.

Methods 2 and 4 for the P and T wave peaks detections (templates combinations) were not tested on the MIT-BIH Arrhythmia database, as the MLII leads from the database's records were used to extract waveform templates by heart cycles clustering.

III. RESULTS

Table 3 is a summary table that shows the average F1 score and the sum of DER for both leads for every method and database. On the left side of the table, the R wave peak

detection methods are given, and on the right side, the P and T wave peaks detection methods are shown. In Tables 4 – 9, we show detailed results of the proposed algorithms for both record leads. Tables 4, 5 and 6 show the total results on the MIT-BIH Arrhythmia Database for R wave, P wave and T wave peaks detections, respectively. Total results on the QT database are shown in Tables 7, 8, and 9, for R wave, P wave, and T wave peaks detections, respectively. The best obtained methods and their results are emphasized (in bold), with the best DER results highlighted in grey.

The computational cost of the methods that showed the best results (in bold and grey in Tables 3 – 9) are shown in Table 10. The presented results are obtained as average from all the considered records in the MIT-BIH Arrhythmia Database. In the second column, the average computation time and standard deviation are presented for each method. Fiducial marks that are detected with the corresponding method are given in brackets. As the Martinez WT + PT method depends both on Martinez's WT and Martinez's PT algorithms, we consider their computation times separately. The template membership rule assignment computation time is averaged on 10 000 RR intervals, and is presented in Table 10, as well.

In Fig. 5, the computation time for different lengths of ECG signals is given for the methods that showed the best results. As the processing steps are computed sequentially, the computation time of each method is presented separately. The methods include: Pan Tompkins (R peak detection), MMF (filtering), Martinez PT, Martinez WT (P, T and R peak detection), Elgendi (R peak detection), and Elgendi (P and T peak detection).

IV. DISCUSSION

We divide this section into several subsections related to different topics. In subsection A, we discuss the metrics used in this work and provide a comparison of the obtained results

TABLE 4. Methods summary performance on MIT-BIH Arrhythmia database (without 102, 104, 107, 207, and 217) for R wave peak detection.

Lead 1								
Method	No. of beats	TP	FP	FN	Se (%)	PPV (%)	F1 (%)	DER (%)
Pan Tompkins (5 - 15)	98873	98435	436	438	99.55	99.55	99.56	0.88
Pan Tompkins (8 - 20)	98873	98280	583	593	99.40	99.41	99.41	1.18
MMF + Pan Tompkins	98873	98113	559	760	99.23	99.43	99.33	1.33
Elgendi	98873	98601	290	272	99.72	99.70	99.72	0.56
MMF + Elgendi	98873	98659	268	214	99.78	99.72	99.76	0.48
MMD + Elgendi	98873	97823	1005	1050	98.93	98.98	98.96	2.07
MMF + MMD + Elgendi	98873	98041	750	832	99.15	99.24	99.20	1.60
Elgendi + Adaptive Thresh.	98873	96981	218	1892	98.08	99.77	98.92	2.13
Martinez WT	98873	97899	6117	974	99.01	94.11	96.50	7.17
MMF + Martinez WT	98873	97284	7392	1589	98.39	92.93	95.59	9.08
MMD+ Martinez WT	98873	95625	6525	3248	96.71	93.61	95.14	9.88
MMD + MMF + Martinez WT	98873	96203	5502	2670	97.29	94.59	95.93	8.26
Lead 2								
Method	No. of beats	TP	FP	FN	Se (%)	PPV (%)	F1 (%)	DER (%)
Pan Tompkins (5 - 15)	98873	88507	7581	10366	89.51	92.11	90.79	18.15
Pan Tompkins (8 - 20)	98873	93314	4918	5559	94.37	94.99	94.68	10.59
MMF + Pan Tompkins	98873	92100	5910	6773	93.14	93.97	93.56	12.82
Elgendi	98873	94847	3852	4026	95.92	96.09	96.01	7.96
MMF + Elgendi	98873	93634	4988	5239	94.70	94.94	94.82	10.34
MMD + Elgendi	98873	93866	4526	5007	94.93	95.40	95.17	9.64
MMF + MMD + Elgendi	98873	94018	4332	4855	95.08	95.59	95.34	9.29
Elgendi + Adaptive Thresh.	98873	90868	3123	8005	91.90	96.67	94.23	11.25
Martinez WT	98873	80182	12375	18691	81.09	86.62	83.77	31.42
MMF + Martinez WT	98873	71229	14508	27644	72.04	83.07	77.17	42.63
MMD+ Martinez WT	98873	88175	15183	10698	89.18	85.31	87.20	26.17
MMD + MMF + Martinez WT	98873	90639	12416	8234	91.67	87.95	89.77	20.88

TABLE 5. Methods summary performance on MIT-BIH Arrhythmia database (without 102, 104, 107, 207, and 217) for P wave peak detection.

Lead 1								
Method	No. of beats	TP	FP	FN	Se (%)	PPV (%)	F1 (%)	DER (%)
Martinez PT	95989	75261	9666	20728	78.41	88.62	83.20	31.66
Martinez WT	95989	70014	16582	25975	72.93	80.85	76.69	44.33
Martinez WT + PT	95989	77318	12172	18671	80.55	86.40	83.37	32.13
Elgendi	95989	59482	38501	36507	61.96	60.70	61.33	78.14
MMF + Elgendi	95989	52948	45770	43041	55.16	53.63	54.39	92.52
MMF + Martinez PT	95989	69586	10175	26403	72.49	87.24	79.19	38.11
MMF + Martinez WT	95989	66111	16699	29878	68.87	79.83	73.95	48.52
MMF + MMD + Martinez WT	95989	46091	28920	49898	48.01	61.44	53.91	82.11
Lead 2								
Method	No. of beats	TP	FP	FN	Se (%)	PPV (%)	F1 (%)	DER (%)
Martinez PT	95989	71117	17800	24872	4.09	9.98	76.92	44.46
Martinez WT	95989	60297	22166	35692	62.81	73.12	67.58	60.27
Martinez WT + PT	95989	72741	17565	23242	75.78	80.55	78.09	42.52
Elgendi	95989	53652	44944	42337	55.89	54.41	55.15	90.92
MMF + Elgendi	95989	43564	55128	52425	45.38	44.14	44.75	112.04
MMF + Martinez PT	95989	69548	18462	26441	72.45	79.02	75.60	46.78
MMF + Martinez WT	95989	58015	23880	37974	60.43	70.84	65.23	64.43
MMF + MMD + Martinez WT	95989	54122	30789	41867	56.38	63.73	59.84	75.69

with related work. In subsection B, a discussion related to R peak detection is provided. Subsection C focuses on the issues related to P and T wave peaks detection. Finally, subsection D is devoted to the discussion on computational burden of the used approaches.

A. COMPARISON TO SIMILAR WORK

To conclude which of the algorithms gave the best solutions overall, we take the DER and F1 score metrics, which both consider the information on the number of TP, FP and FN

detections in a signal and thus can be considered as the most comprehensive evaluation measures. When DER tends to decrease, F1 score tends to increase. In Table 3, the best methods in terms of F1 score coincide with the best methods in terms of DER. Since there is no clear benefit in discussing both evaluation metrics that behave in the same way, in further text, the results are discussed in terms of DER. Due to the observed inconsistency in the annotations for P and T wave peaks (some of the peaks are clearly missed), we also discuss the algorithms in terms of sensitivity (Se), as Se does not

TABLE 6. Methods summary performance on MIT-BIH Arrhythmia database (without 102, 104, 107, 207, and 217) for T wave peak detection.

Lead 1								
Method	No. of beats	TP	FP	FN	Se (%)	PPV (%)	F1 (%)	DER (%)
Martinez PT	98395	71583	22636	26812	72.75	75.97	74.33	50.25
Martinez WT	98395	66071	29210	32324	67.14	69.34	68.23	62.53
Martinez WT + PT	98395	70007	27352	28388	71.14	71.90	71.53	56.64
Elgendi	98395	87810	5569	10585	89.24	94.03	91.58	16.41
MMF + Elgendi	98395	88894	6310	9501	90.34	93.37	91.83	16.06
MMF + Martinez PT	98395	62105	32952	36290	63.11	65.33	64.21	70.37
MMF + Martinez WT	98395	61490	29040	36905	62.49	67.92	65.09	67.02
MMF + MMD + Martinez WT	98395	46939	37493	51456	47.70	55.59	51.35	90.39
Lead 2								
Method	No. of beats	TP	FP	FN	Se (%)	PPV (%)	F1 (%)	DER (%)
Martinez PT	98395	57225	35678	41170	58.15	61.59	59.83	78.10
Martinez WT	98395	58132	35085	40263	59.08	62.36	60.68	76.57
Martinez WT + PT	98395	58061	37946	40334	59.00	60.47	59.73	79.55
Elgendi	98395	46683	45819	51712	47.44	50.46	48.91	99.12
MMF + Elgendi	98395	50273	45129	48122	51.09	52.69	51.88	94.77
MMF + Martinez PT	98395	57642	37626	40753	58.58	60.50	59.53	79.65
MMF + Martinez WT	98395	55877	36692	42518	56.78	60.36	58.52	80.50
MMF + MMD + Martinez WT	98395	48105	38789	50290	48.88	55.36	51.92	90.53

TABLE 7. Methods summary performance on QT database (with reannotated record sel232) for R wave peak detection.

Lead 1								
Method	No. of beats	TP	FP	FN	Se (%)	PPV (%)	F1 (%)	DER (%)
Pan Tompkins (5 - 15)	86357	84726	2386	1631	98.11	97.26	97.68	4.65
Pan Tompkins (8 - 20)	86357	84781	2198	1576	98.17	97.47	97.82	4.37
MMF + Pan Tompkins	86357	84849	2161	1508	98.25	97.51	97.88	4.24
Elgendi	86357	84865	3304	1492	98.27	96.25	97.25	5.55
MMF + Elgendi	86357	84618	2545	1739	97.98	97.08	97.53	4.96
MMD + Elgendi	86357	74056	14270	12301	85.75	83.84	84.79	30.76
MMF + MMD + Elgendi	86357	79777	7401	6580	92.38	91.51	91.94	16.18
Elgendi + Adaptive Thresh.	86357	84445	3073	1912	97.78	96.48	97.13	5.77
Martinez WT	86357	84648	6802	1709	98.02	92.56	95.21	9.85
MMF + Martinez WT	86357	83946	11991	2411	97.20	87.50	92.10	16.67
MMD + Martinez WT	86357	83774	8462	2583	97.01	90.82	93.82	12.78
MMD + MMF + Martinez WT	86357	83882	8515	2475	97.13	90.78	93.85	12.72
Lead 2								
Method	No. of beats	TP	FP	FN	Se (%)	PPV (%)	F1 (%)	DER (%)
Pan Tompkins (5 - 15)	86357	81719	5886	4638	94.62	93.28	93.95	12.18
Pan Tompkins (8 - 20)	86357	84061	3357	2296	97.34	96.15	96.75	6.54
MMF + Pan Tompkins	86357	84219	3731	2138	97.52	95.75	96.63	6.79
Elgendi	86357	84230	4938	2127	97.53	94.46	95.97	8.18
MMF + Elgendi	86357	84775	3113	1582	98.16	96.45	97.31	5.43
MMD + Elgendi	86357	80426	8292	5931	93.13	90.65	91.88	16.47
MMF + MMD + Elgendi	86357	82841	5029	3516	95.92	94.27	95.10	9.89
Elgendi + Adaptive Thresh.	86357	84025	3987	2332	97.29	95.46	96.38	7.31
Martinez WT	86357	77152	8140	9205	89.34	90.45	89.90	20.08
MMF + Martinez WT	86357	69715	10035	16642	80.72	87.41	83.94	30.89
MMD + Martinez WT	86357	82470	9682	3887	95.49	89.49	92.40	15.71
MMD + MMF + Martinez WT	86357	84178	7902	2179	97.47	91.41	94.35	11.67

incorporate false positive detections, which are maybe missed because of the annotations.

The results of our research differs significantly from those presented in literature (compare the results shown in Table 1 with Tables 3–9), especially in the cases of P and T wave peaks detection. We suspect this is due to the following reasons:

- 1) our lower (more strict) sample deviation interval, based on AAMI ECAR guidelines (e.g. in [25], sample deviation interval of 120 ms was used)

- 2) inconsistent annotations from multiple annotators can lead to different interpretations [31],
- 3) other researchers report only the best lead results, which may not be representative in a real case scenario where the actual sample of peak occurrence is unknown [25], and
- 4) the exact protocol of determining the true positive P and T wave peak detection is not described in some of the related work [30], [32], which reduces reproducibility of the results.

TABLE 8. Methods summary performance on QT database (with reannotated record sel232) for P wave peak detection.

Lead 1								
Method	No. of beats	TP	FP	FN	Se (%)	PPV (%)	F1 (%)	DER (%)
Martinez PT	3194	2859	342	335	89.51	89.32	89.41	21.20
Martinez PT + templates	3194	2816	320	378	88.17	89.90	88.97	21.85
Martinez WT	3194	2739	499	455	85.75	84.58	85.17	29.86
Martinez WT + templates	3194	2751	395	443	86.13	87.44	86.78	26.23
Martinez WT + PT	3194	2932	416	262	91.80	87.57	89.64	21.23
Elgendi	3194	2392	1187	802	74.89	66.83	70.63	62.27
MMF + Elgendi	3194	1572	2029	1622	49.21	43.65	46.27	114.30
MMF + Martinez PT	3194	2501	442	693	78.30	84.98	81.51	35.54
MMF + Martinez WT	3194	2370	557	824	74.20	80.97	77.44	43.23
MMF + MMD + Martinez WT	3194	2117	954	1077	66.28	68.93	67.58	63.58
Lead 2								
Method	No. of beats	TP	FP	FN	Se (%)	PPV (%)	F1 (%)	DER (%)
Martinez PT	3194	2751	472	443	86.13	85.36	85.74	28.65
Martinez PT + templates	3194	2752	467	442	86.16	85.49	85.83	28.46
Martinez WT	3194	2733	442	461	85.56	86.07	85.82	28.27
Martinez WT + templates	3194	2747	392	447	86.01	87.51	86.75	26.27
Martinez WT + PT	3194	2845	507	349	89.07	84.87	86.92	26.80
Elgendi	3194	2329	1286	865	72.91	64.42	68.41	67.34
MMF + Elgendi	3194	1433	2186	1761	44.86	39.59	42.07	123.57
MMF + Martinez PT	3194	2551	593	643	79.87	81.14	80.50	38.70
MMF + Martinez WT	3194	2285	591	909	71.54	79.45	75.29	46.96
MMF + MMD + Martinez WT	3194	2379	770	815	74.48	75.54	75.01	49.62

TABLE 9. Methods summary performance on QT database (with reannotated record sel232) for T wave peak detection.

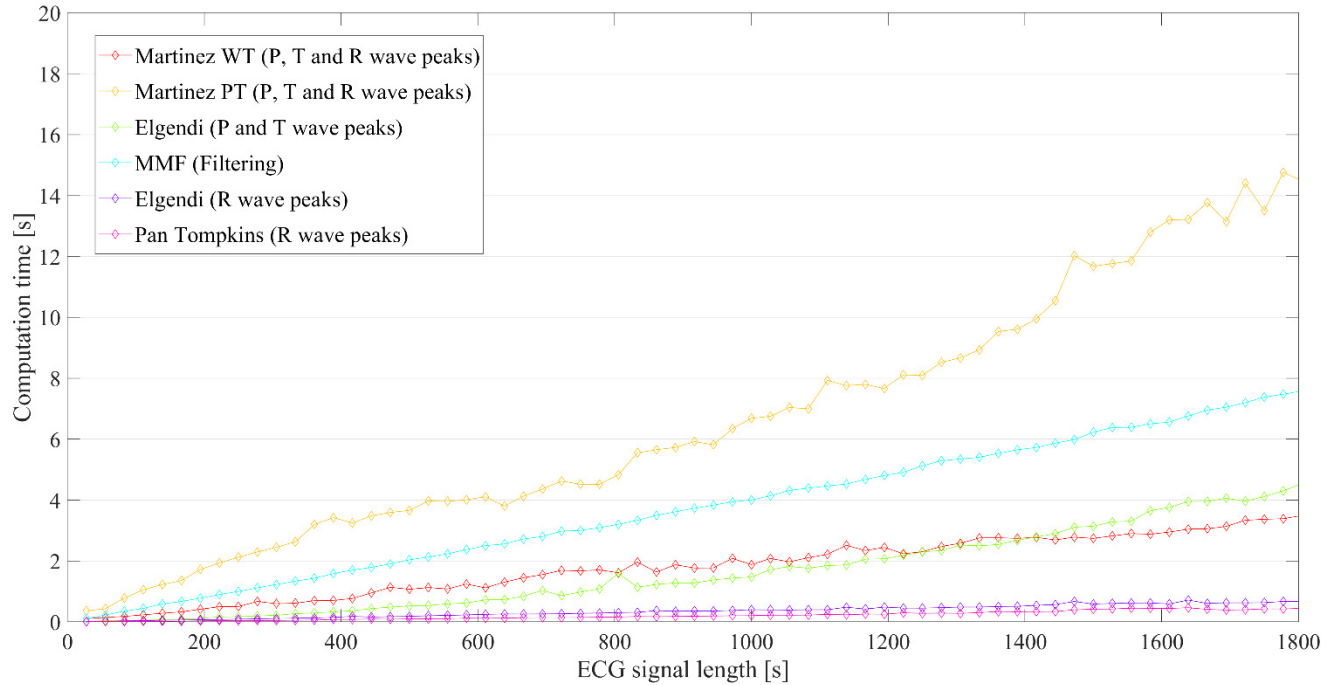
Lead 1								
Method	No. of beats	TP	FP	FN	Se (%)	PPV (%)	F1 (%)	DER (%)
Martinez PT	3542	2985	559	557	84.27	84.22	84.25	31.50
Martinez PT + templates	3542	3035	505	507	85.68	85.73	85.71	28.57
Martinez WT	3542	3087	475	455	87.15	86.66	86.91	26.25
Martinez WT + templates	3542	3115	464	427	87.94	87.03	87.49	25.15
Martinez WT + PT	3542	3030	558	512	85.54	84.44	84.99	30.20
Elgendi	3542	2632	942	910	74.30	73.64	73.97	52.28
MMF + Elgendi	3542	2720	884	822	76.79	75.47	76.13	48.16
MMF + Martinez PT	3542	3007	569	535	84.89	84.08	84.49	31.16
MMF + Martinez WT	3542	2947	562	595	83.20	83.98	83.59	32.66
MMF + MMD + Martinez WT	3542	2332	1038	1210	65.83	69.19	67.48	63.46
Lead 2								
Method	No. of beats	TP	FP	FN	Se (%)	PPV (%)	F1 (%)	DER (%)
Martinez PT	3542	2888	580	654	81.53	83.27	82.40	34.83
Martinez PT + templates	3542	2905	565	637	82.01	83.71	82.86	33.93
Martinez WT	3542	3113	383	429	87.88	89.04	88.46	22.92
Martinez WT + templates	3542	3114	381	428	87.91	89.09	88.50	22.84
Martinez WT + PT	3542	3012	557	530	85.03	84.39	84.71	30.68
Elgendi	3542	2816	722	726	79.50	79.59	79.55	40.88
MMF + Elgendi	3542	2855	743	687	80.60	79.34	79.97	40.37
MMF + Martinez PT	3542	3055	508	487	86.25	85.74	86.00	28.09
MMF + Martinez WT	3542	3037	380	505	85.74	88.87	87.28	24.98
MMF + MMD + Martinez WT	3542	2623	746	919	74.05	77.85	75.91	47.00

The problem of different sample deviation intervals for evaluation is discussed in [11]. In [11], a range of sample error intervals were tested, with the reported results for P and T wave peak detections in line with ours (Se is around and below 90% for P wave peak detection and below 80% for T wave peak detection with ± 80 ms sample deviation interval on the algorithms tested on QT Database). However, note that putting aside the absolute values of the results, our work mainly focuses on discovering whether the combinations of processing steps increase the detection accuracy compared

to the original methods. In this setting, we emphasize that the evaluation protocol has been the same for all the tested methods, so we can compare the increase (or decrease) in DER and Se.

B. DETECTION OF R PEAKS

For QRS complex (R peak) detection, when comparing the results on both leads (Table 3), method 3 (Elgendi's algorithm) gave the best results regarding DER on the MIT-BIH Arrhythmia Database. However, using MMF with Elgendi's

**FIGURE 5.** Method computation times for different ECG signal lengths.**TABLE 10.** The average computation time for each algorithm on 30-minute long ECG recordings.

Method	Computation time [s]
Elgendi (P, T and R wave peaks)	4.859 ± 1.098
MMF + Elgendi (P, T and R wave peaks)	13.290 ± 1.167
MMF + Pan Tompkins (R peak)	8.037 ± 0.500
Martinez WT (P, T and R wave peaks)	18.453 ± 13.113
Martinez PT (P, T and R wave peaks)	52.671 ± 50.963
Template membership rule assignment ^a	0.079 ± 0.029

^aThe average computation time for a single RR interval

algorithm improved the results on the QT Database. When considering only the first lead, the combinations of MMF and Elgendi's algorithm (on MIT-BIH Arrhythmia Database), and MMF and Pan Tompkins' algorithm (on QT Database) show the best overall results.

It is noted that the MMF noise reduction proposed by [34] works well only on some of the records, while on some others, it lowers the expected accuracy. We suspect that the lower results on some records are caused by the fact that the structuring elements of MMF are fixed and based on *a priori* knowledge. Thus, in some cases, MMF can filter out useful information about characteristic waves, which can result in a higher DER than when MMF is not applied. Although the number of cases like this is small, overall improvement of QRS detection when MMF is used (Table 3) is lower than expected. In [47], an algorithm based on adaptive mathematical morphology is proposed, which gave promising results.

With this approach, the structuring elements of MMF can be modified for each recording so that no information about the waves are lost or degraded. Using the adaptive thresholding of Pan Tompkins' algorithm with Elgendi's algorithm improved the overall PPV, as expected, but the Se and DER degraded, as there is a high increase in FN detection, due to added additional thresholding step. Higher Se was achieved when the first lead (MLII) was used, possibly because of the high amplitude QRS complexes in that lead.

According to the results on both leads, Elgendi's algorithm alone, or in the combination with MMF, is the best R wave peak detector. However, it should be noted that the Elgendi's algorithm is optimized for the MIT-BIH Arrhythmia Database. This would mean that, if we disregard the Elgendi's algorithm results on the MIT-BIH Arrhythmia Database due to the optimization bias, the Elgendi + MMF combination is shown to be the most accurate R wave peak detector. This finding could mean that the Elgendi's algorithm should be used in combination with MMF in general. Note that this assumption should be verified on other ECG databases with R wave peak annotations.

C. DETECTION OF P AND T WAVE PEAKS

Martinez's PT algorithm shows the best results for P wave peak detection on both databases, with the lowest DER when using only the first lead. Slight improvement in Se of the detection may be obtained when the PT algorithm is combined with Martinez's WT algorithm. In addition, when both of the leads are considered, the combination of PT and

WT algorithms gave the lowest sum of DER on both databases, which is an important result.

On the MIT-BIH Arrhythmia Database, the combination of MMF and Elgendi's algorithm gave the best results for T wave peak detection (on the first lead and on the sum of both leads). For the QT database, Martinez's WT algorithm in combination with templates shows the best results. From Table 9, we can see that the second lead is better for the detection of T wave peaks than the first lead, although in most of the described algorithms, only the first lead is used. This suggests that the detection of this characteristic wave is lead dependent. If more than one ECG lead are available, automatic lead selection should be incorporated, if possible, in order to determine the optimal lead for desired characteristic wave detection (for example, based on the first 30 seconds of the signal [48]).

It is important to mention that P and T wave peaks annotations of the MIT-BIH Arrhythmia Database made publicly available by Li *et al.* [35] do not match those in the QT Database for the same records (*sel100*, *sel102*, *sel103*, *sel104*, *sel114*, *sel116*, *sel117*, *sel123*, *sel213*, *sel221*, *sel223*, *sel230*, *sel231*, *sel232* and *sel233*). In our opinion, the annotations of P and T waves in the QT Database are the better ones, because Elgendi *et al.* [41] often did not annotate the inverted T waves, which is visible when inspecting both leads. If the T waves are approximately biphasic on a single lead, the positive wave is frequently selected, despite the fact that the negative wave may have a larger amplitude than the positive one and without consideration for the T wave on the other lead. Elgendi's method selects the highest positive peak in a block of interest. Therefore, there is a reason to believe that Elgendi's T wave annotations are biased in the respect described above.

Generally speaking, our opinion, based on the conducted work, is that Martinez's WT algorithm is the best T wave peak detector. Note that we show that T wave peak detection accuracy is further enhanced by using the search window parameter modification for RR intervals that belong to a particular waveform template (see Table 9).

D. COMPUTATION TIME

As the length of ECG records can be quite long, it is important to consider the computational cost of the proposed methods. From Table 10, it can be seen that Martinez's PT is considerably more time demanding than Elgendi's or Martinez's WT methods. Also, the average computation time on 30-minute long ECG recordings is considerably longer when MMF processing step is used. The MMF method has an approximately linear computational complexity (see Fig. 5) and for the input ECG signal that is 30 minutes long, it runs up to 8 seconds. Methods combined with MMF are therefore considerably longer in duration, especially when long ECG records are analyzed. Optimized versions of some of the algorithms, for example, fast MMF algorithm, may be used to achieve more efficient MMF computations [49].

The average computation time of template membership rule assignment for a single RR interval is 0.079 s (Table 10).

On 30-minute long ECG recordings, with an average heart rate of 60 bpm, this can prolong the calculation for about 142 seconds, which may not be suitable for real-time detection purposes. However, if the RR interval is assigned to a current template, P and T wave peaks detection is done by comparing the membership rules of the assigned template. The number of RR intervals that gets assigned to current templates depends on the morphology of the signal. In our case, about 60% of the RR intervals is assigned to the templates. In terms of P and T wave peak detections, this can yield a significant computation time improvement.

Holter ECG recordings are usually up to 48 hours long. The computations that take more than several minutes can be impractical in everyday use, and a compromise between the computational burden and detection accuracy is an important factor to consider in such cases. When we examine the acceptability of the methods for real-time use, Elgendi's methods are the most suitable for R peak detections, as most of the methods have high accuracy. For T and P wave peak detections, although with a lower accuracy than some of the other methods, Elgendi's method may be used if fast computation time is required. However, we believe that the importance of accurate detection overcomes the computational cost, especially in the cases where the computation time grows approximately linearly with respect to the record length (see Fig. 5). Hence, MMF preprocessing step as well as Martinez's algorithms (including our modified PT algorithm) may also be considered for real-time uses, when highly accurate detection of peaks is sought.

V. CONCLUSION

In this paper, we combined methods from several known algorithms for detection of characteristic waves in ECG. Detection of QRS complexes achieved high sensitivity and positive predictive value. The proposed modifications showed some improvement over QRS detection methods (Elgendi's method) when additional noise and artefact reduction step (MMF) was used. The improvement with the use of MMF suggests that special cases of signal distortion are causing false detections. Although slight improvements may be achieved using the same method for T wave peak detection (see the results for method 7 on the MIT-BIH Arrhythmia Database), we do not advise the same combination for P wave peak detection. However, in future work, we plan to incorporate adaptive MMF for each recording to insure the optimal MMF structuring element that will preserve information about all the characteristic waves, which could lead to further improvements of the results. We consider that the adaptive approach may improve algorithm detections in the case of abnormal ECG cycles (such as the presence of PVC and paced beats or presence of flutter waves), when the morphology of ECG waves is drastically changed.

We have shown that the modified Martinez's PT algorithm proved the best for P wave peak detection and that Martinez's WT in combination with waveform templates extracted by heart cycles clustering reached the best results for T wave

peak detections. Nevertheless, both sensitivity and positive predictive value are still around or less than 90% for P and T wave peaks detection. In an effort to improve P and T wave detection algorithms, high quality annotated databases are still lacking. We would like to encourage medical experts to help annotate the publicly available ECG databases, as the value of contemporary high accuracy algorithms can only be established on well-annotated datasets. As acquiring ECGs from subjects is not an issue nowadays, due to advanced remote monitoring systems [50], we consider that reserving some expert time to annotate and publish the acquired signals is crucial for further advancements in automatic detection algorithms.

Parameter modification of Martinez's PT algorithm based on waveform templates extracted by heart cycles clustering used in this work is still under development. Perhaps the membership of the RR intervals to certain templates could be described better with different or somewhat modified membership rules. We suppose that the accuracy of P and T waves detection could be further enhanced by concentrating the templates, along with the membership rules, to the P and T waves' onset, peak and offset, respectively. This application of templates may insure high quality extraction of clinically relevant ECG features, like QT and PR intervals.

The computational burden of different methods is briefly explored in this paper. However, it is important to note that our algorithms are implemented in Matlab, with some parts implemented in C++, which may not help in clarifying all the details regarding their comparison. Hence, although we showed experimentally that most of the methods considered in this work may be used in real-time applications, further, more detailed, studies focusing on computational complexity of the methods may provide a clearer insight.

ACKNOWLEDGMENT

The authors would like to thank Sinisa Car, MD, for his valuable assistance with the diagnostic characteristics related to ECG morphology.

REFERENCES

- [1] A. Gacek and W. Pedrycz, Eds., *ECG Signal Processing, Classification and Interpretation: A Comprehensive Framework of Computational Intelligence*. London, U.K.: Springer, 2012, doi: [10.1007/978-0-85729-868-3](https://doi.org/10.1007/978-0-85729-868-3).
- [2] A. Jovic, D. Kukolja, K. Friganovic, K. Jozic, and S. Car, "Biomedical time series preprocessing and expert-system based feature extraction in MULTISAB platform," in *Proc. MIPRO*, Opatija, Croatia, 2017, pp. 349–354.
- [3] R. Sassi et al., "Advances in heart rate variability signal analysis: Joint position statement by the E-cardiology ESC working group and the European heart rhythm association co-endorsed by the asia pacific heart rhythm society," *Europace*, vol. 17, no. 9, pp. 1341–1353, 2015, doi: [10.1093/europace/euv015](https://doi.org/10.1093/europace/euv015).
- [4] Y. Miao, Y. Tian, L. Peng, M. S. Hossain, and G. Muhammad, "Research and implementation of ECG-based biological recognition parallelization," *IEEE Access*, vol. 6, pp. 4759–4766, 2018, doi: [10.1109/ACCESS.2017.2771220](https://doi.org/10.1109/ACCESS.2017.2771220).
- [5] J. Pan and W. J. Tompkins, "A real-time QRS detection algorithm," *IEEE Trans. Biomed. Eng.*, vol. BME-32, no. 3, pp. 230–236, Mar. 1985, doi: [10.1109/TBME.1985.325532](https://doi.org/10.1109/TBME.1985.325532).
- [6] M. Elgendi, "Fast QRS detection with an optimized knowledge-based method: Evaluation on 11 standard ECG databases," *PLoS ONE*, vol. 8, no. 9, e73557, 2013, doi: [10.1371/journal.pone.0073557](https://doi.org/10.1371/journal.pone.0073557).
- [7] G. D. Clifford, F. Azuaje, and P. McSharry, *Advanced Methods and Tools for ECG Data Analysis*. Boston, MA, USA: Artech House, 2006.
- [8] J. Kim and H. Shin, "Simple and robust realtime QRS detection algorithm based on spatiotemporal characteristic of the QRS complex," *PLoS ONE*, vol. 11, no. 3, p. e0150144, 2016, doi: [10.1371/journal.pone.0150144](https://doi.org/10.1371/journal.pone.0150144).
- [9] S. Pal and M. Mitra, "Empirical mode decomposition based ECG enhancement and QRS detection," *Comput. Biol. Med.*, vol. 42, pp. 83–92, Jan. 2012, doi: [10.1016/j.combiomed.2011.10.012](https://doi.org/10.1016/j.combiomed.2011.10.012).
- [10] M. S. Manikandan and K. P. Soman, "A novel method for detecting R-peaks in electrocardiogram (ECG) signal," *Biomed. Signal Process. Control*, vol. 7, no. 2, pp. 118–128, 2012, doi: [10.1016/j.bspc.2011.03.004](https://doi.org/10.1016/j.bspc.2011.03.004).
- [11] H. Leutheuser et al., "Instantaneous P- and T-wave detection: Assessment of three ECG fiducial points detection algorithms," in *Proc. 13th Annu. Body Sens. Netw. Conf.*, San Francisco, CA, USA, 2016, pp. 329–334, doi: [10.1109/BSN.2016.7516283](https://doi.org/10.1109/BSN.2016.7516283).
- [12] M. Talbi, A. Aouinet, R. Baazaoui, and A. Cherif, "ECG analysis based on wavelet transform and modulus maxima," *Int. J. Comput. Sci. Issues*, vol. 9, no. 1, pp. 427–435, 2012.
- [13] C. Alvarado, J. Arregui, J. Ramos, and R. Pallàs-Areny, "Automatic detection of ECG ventricular activity waves using continuous spline wavelet transform," in *Proc. 2nd Int. Conf. Electr. Electron. Eng.*, Mexico City, Mexico, 2005, pp. 189–192, doi: [10.1109/ICEEEE.2005.1529605](https://doi.org/10.1109/ICEEEE.2005.1529605).
- [14] M. Boix, B. Cantó, D. Cuesta, and P. Micó, "Using the wavelet transform for T-wave alternans detection," *Math. Comput. Model.*, vol. 50, pp. 738–742, Sep. 2009, doi: [10.1016/j.mcm.2009.05.002](https://doi.org/10.1016/j.mcm.2009.05.002).
- [15] A. Ghaffari, M. R. Homaeinezhad, M. Khazraee, and M. M. Daevaeiha, "Segmentation of holter ECG waves via analysis of a discrete wavelet-derived multiple skewness-kurtosis based metric," *Ann. Biomed. Eng.*, vol. 38, no. 4, pp. 1497–1510, 2010, doi: [10.1007/s10439-010-9919-3](https://doi.org/10.1007/s10439-010-9919-3).
- [16] D. S. Benitez, P. A. Gaydecki, A. Zaidi, and A. P. Fitzpatrick, "A new QRS detection algorithm based on the Hilbert transform," in *Proc. Comput. Cardiol.*, Boston, MA, USA, vol. 27, 2000, pp. 379–382, doi: [10.1109/CIC.2000.898536](https://doi.org/10.1109/CIC.2000.898536).
- [17] D. Benitez, P. A. Gaydecki, A. Zaidi, and A. P. Fitzpatrick, "The use of the Hilbert transform in ECG signal analysis," *Comput. Biol. Med.*, vol. 31, no. 5, pp. 399–406, 2001, doi: [10.1016/S0010-4825\(01\)00009-9](https://doi.org/10.1016/S0010-4825(01)00009-9).
- [18] J. P. Madeiro, P. C. Cortez, J. A. Marques, C. R. Seisdedos, and C. R. Sobrinho, "An innovative approach of QRS segmentation based on first-derivative, Hilbert and wavelet transforms," *Med. Eng. Phys.*, vol. 34, no. 9, pp. 1236–1246, 2012, doi: [10.1016/j.medengphy.2011.12.011](https://doi.org/10.1016/j.medengphy.2011.12.011).
- [19] H. Li, X. Wang, L. Chen, and E. Li, "Denoising and R-peak detection of electrocardiogram signal based on EMD and improved approximate envelope," *Circuits, Syst., Signal Process.*, vol. 33, no. 4, pp. 1261–1276, 2014, doi: [10.1007/s00034-013-9691-3](https://doi.org/10.1007/s00034-013-9691-3).
- [20] H. Li and X. Wang, "Detection of electrocardiogram characteristic points using lifting wavelet transform and Hilbert transform," *Trans. Inst. Meas. Control*, vol. 35, no. 5, pp. 574–582, 2013, doi: [10.1177/0142331212460720](https://doi.org/10.1177/0142331212460720).
- [21] S. Kiranyaz, T. Ince, and M. Gabbouj, "Real-time patient-specific ECG classification by 1-D convolutional neural networks," *IEEE Trans. Biomed. Eng.*, vol. 63, no. 3, pp. 664–675, Mar. 2016, doi: [10.1109/TBME.2015.2468589](https://doi.org/10.1109/TBME.2015.2468589).
- [22] B. Abibullaev and H. D. Seo, "A new QRS detection method using wavelets and artificial neural networks," *J. Med. Syst.*, vol. 35, no. 4, pp. 683–691, 2011, doi: [10.1007/s10916-009-9405-3](https://doi.org/10.1007/s10916-009-9405-3).
- [23] K. Friganovic, A. Jovic, D. Kukolja, M. Cifrek, and G. Krstacic, "Optimizing the detection of characteristic waves in ECG based on exploration of processing steps combinations," in *Proc. IFMBE Conf. EMBEC NBC*, Tampere, Finland, 2017, pp. 928–932, doi: [10.1007/978-981-10-5122-7_232](https://doi.org/10.1007/978-981-10-5122-7_232).
- [24] K. Friganovic, A. Jovic, K. Jozic, D. Kukolja, and M. Cifrek, "MULTISAB project: A Web platform based on specialized frameworks for heterogeneous biomedical time series analysis—An architectural overview," in *Proc. CMBEIH*, Sarajevo, Bosnia and Herzegovina, 2017, pp. 9–15, doi: [10.1007/978-981-10-4166-2_2](https://doi.org/10.1007/978-981-10-4166-2_2).
- [25] I. Beraza and I. Romero, "Comparative study of algorithms for ECG segmentation," *Biomed. Signal Process. Control*, vol. 34, pp. 166–173, Apr. 2017, doi: [10.1016/j.bspc.2017.01.013](https://doi.org/10.1016/j.bspc.2017.01.013).
- [26] C. R. Vázquez-Seisdedos, J. E. Neto, E. J. M. Reyes, A. Klautau, and R. C. L. de Oliveira, "New approach for T-wave end detection on electrocardiogram: Performance in noisy conditions," *Biomed. Eng. Online*, vol. 10, p. 77, Sep. 2011, doi: [10.1186/1475-925X-10-77](https://doi.org/10.1186/1475-925X-10-77).

- [27] M. Vítek, J. Hubreš, and J. Kozumplík, "A wavelet-based ECG delineation with improved P wave offset detection accuracy," in *Proc. 20th Int. EURASIP Conf. Biosignal*, Brno, Czech Republic, Jun. 2010, pp. 160–165.
- [28] Y. N. Singh and P. Gupta, "ECG to individual identification," in *Proc. 2nd IEEE Int. Conf. Biometrics, Theory, Appl. Syst. (BTAS)*, Washington, DC, USA, Sep./Oct. 2008, pp. 1–8.
- [29] L. Y. Di Marco and L. Chiari, "A wavelet-based ECG delineation algorithm for 32-bit integer online processing," *Biomed. Eng. Online*, vol. 10, p. 23, Apr. 2011, doi: [10.1186/1475-925X-10-23](https://doi.org/10.1186/1475-925X-10-23).
- [30] M. Elgendi, M. Meo, and D. Abbott, "A proof-of-concept study: Simple and effective detection of P and T waves in arrhythmic ECG signals," *Bioengineering*, vol. 3, no. 4, p. 26, 2016, doi: [10.3390/bioengineering3040026](https://doi.org/10.3390/bioengineering3040026).
- [31] J. P. Martinez, R. Almeida, S. Olmos, A. P. Rocha, and P. Laguna, "A wavelet-based ECG delineator: Evaluation on standard databases," *IEEE Trans. Biomed. Eng.*, vol. 51, no. 4, pp. 570–581, Apr. 2004, doi: [10.1109/TBME.2003.821031](https://doi.org/10.1109/TBME.2003.821031).
- [32] Y. Sun, K. L. Chan, and S. M. Krishnan, "Characteristic wave detection in ECG signal using morphological transform," *BMC Cardiovascular Disorders*, vol. 5, p. 28, Sep. 2005, doi: [10.1186/1471-2261-5-28](https://doi.org/10.1186/1471-2261-5-28).
- [33] A. Martinez, R. Alcaraz, and J. J. Rieta, "A new method for automatic delineation of ECG fiducial points based on the phasor transform," in *Proc. Annu. Int. Conf. IEEE Eng. Med. Biol. Soc. (EMBC)*, Buenos Aires, Argentina, 2010, pp. 4586–4589, doi: [10.1109/EMBS.2010.5626498](https://doi.org/10.1109/EMBS.2010.5626498).
- [34] Y. Sun, K. L. Chan, and S. M. Krishnan, "ECG signal conditioning by morphological filtering," *Comput. Biol. Med.*, vol. 32, no. 6, pp. 465–479, Nov. 2002, doi: [10.1016/S0010-4825\(02\)00034-3](https://doi.org/10.1016/S0010-4825(02)00034-3).
- [35] C. Li, C. Zheng, and C. Tai, "Detection of ECG characteristic points using wavelet transforms," *IEEE Trans. Biomed. Eng.*, vol. 42, no. 1, pp. 21–28, Jan. 1995, doi: [10.1109/10.362922](https://doi.org/10.1109/10.362922).
- [36] S. Mallat and S. Zhong, "Characterization of signals from multi-scale edges," *IEEE Trans. Pattern Anal. Mach. Intell.*, vol. 14, no. 7, pp. 710–732, Jul. 1992, doi: [10.1109/34.142909](https://doi.org/10.1109/34.142909).
- [37] R. A. Álvarez, A. J. M. Penin, and X. A. V. Sobrino, "A comparison of three QRS detection algorithms over a public database," *Procedia Technol.*, vol. 9, pp. 1159–1165, 2013, doi: [10.1016/j.protcy.2013.12.129](https://doi.org/10.1016/j.protcy.2013.12.129).
- [38] G. B. Moody and R. G. Mark, "The impact of the MIT-BIH arrhythmia database," *IEEE Eng. Med. Biol. Mag.*, vol. 20, no. 3, pp. 45–50, May/Jun. 2001, doi: [10.1109/51.932724](https://doi.org/10.1109/51.932724).
- [39] P. Laguna, R. G. Mark, A. Goldberg, and G. B. Moody, "A database for evaluation of algorithms for measurement of QT and other waveform intervals in the ECG," in *Proc. Comput. Cardiol.*, Boston, MA, USA, vol. 24, 1997, pp. 673–676, doi: [10.1109/CIC.1997.648140](https://doi.org/10.1109/CIC.1997.648140).
- [40] A. L. Goldberger et al., "PhysioBank, PhysioToolkit, and PhysioNet: Components of a new research resource for complex physiologic signals," *Circulation*, vol. 101, no. 23, pp. e215–e220, 2000, doi: [10.1161/01.CIR.101.23.e215](https://doi.org/10.1161/01.CIR.101.23.e215).
- [41] M. Elgendi, B. Eskofier, and D. Abbott, "Fast T wave detection calibrated by clinical knowledge with annotation of P and T waves," *Sensors*, vol. 15, no. 7, pp. 17693–17714, 2015, doi: [10.3390/s150717693](https://doi.org/10.3390/s150717693).
- [42] M. R. Homaeinezhad, M. ErfanianMoshiri-Nejad, and H. Naseri, "A correlation analysis-based detection and delineation of ECG characteristic events using template waveforms extracted by ensemble averaging of clustered heart cycles," *Comput. Biol. Med.*, vol. 44, pp. 66–75, Jan. 2014, doi: [10.1016/j.combiomed.2013.10.024](https://doi.org/10.1016/j.combiomed.2013.10.024).
- [43] J. Yang and J. Leskovec, "Patterns of temporal variation in online media," in *Proc. 4th ACM Int. Conf. Web Search Data Mining (WSDM)*, Hong Kong, 2011, pp. 177–186, doi: [10.1145/1935826.1935863](https://doi.org/10.1145/1935826.1935863).
- [44] F. N. Fritsch and R. E. Carlson, "Monotone piecewise cubic interpolation," *SIAM J. Numer. Anal.*, vol. 17, no. 2, pp. 238–246, 1980, doi: [10.1137/0717021](https://doi.org/10.1137/0717021).
- [45] D. Kahaner, C. Moler, and S. Nash, *Numerical Methods and Software*. Upper Saddle River, NJ, USA: Prentice-Hall, 1989.
- [46] AAMI-ECAR, *Recommended Practice for Testing and Reporting Performance Results of Ventricular Arrhythmia Detection Algorithms*. Arlington, VA, USA: Association for the Advancement of Medical Instrumentation, 1987.
- [47] S. Yazdani and J.-M. Vesin, "Extraction of QRS fiducial points from the ECG using adaptive mathematical morphology," *Digit. Signal Process.*, vol. 56, pp. 100–109, Sep. 2016, doi: [10.1016/j.dsp.2016.06.010](https://doi.org/10.1016/j.dsp.2016.06.010).
- [48] W. Zong, M. Saeed, and T. Heldt, "A QT interval detection algorithm based on ECG curve length transform," in *Proc. Comput. Cardiol.*, Boston, MA, USA, 2006, pp. 377–380.
- [49] Y. Chou, B. Xu, Y. Gu, R. Zhang, L. Wang, and Y. Jin, "A fast mathematical morphology filter on one dimensional sampled signal," in *Proc. Int. Conf. Control, Automat. Inf. Sci. (ICCAIS)*, Chiang Mai, Thailand, 2017, pp. 233–238, doi: [10.1109/ICCAIS.2017.8217582](https://doi.org/10.1109/ICCAIS.2017.8217582).
- [50] M. Hooshmand, D. Zordan, T. Melodia, and M. Rossi, "SURF: Subject-adaptive unsupervised ECG signal compression for wearable fitness monitors," *IEEE Access*, vol. 5, pp. 19517–19535, 2017, doi: [10.1109/ACCESS.2017.2749758](https://doi.org/10.1109/ACCESS.2017.2749758).



KRESIMIR FRIGANOVIC received the M.Sc. degree from the Faculty of Electrical Engineering and Computing, University of Zagreb, Croatia, in 2016, where he is currently pursuing the Ph.D. degree. He is currently a Research Assistant with the University of Zagreb, where he is currently involved in the MULTISAB Project developing a software system for parallel analysis of multiple heterogeneous time series with applications in biomedicine.

His research interests include biomedical signal processing, EEG and ECG signal analysis, and machine learning applications.



DAVOR KUKOLJA received the B.Sc. degree in electrical engineering and the Ph.D. degree in computer science from the Faculty of Electrical Engineering and Computing, University of Zagreb, Zagreb, Croatia, in 2005 and 2014, respectively.

He was a Research Assistant and a Teaching Assistant with the Department of Electric Machines, Drives and Automation, Faculty of Electrical Engineering and Computing, University of Zagreb, from 2006 to 2016, where he was a Post-Doctoral Researcher with the Department of electronics, microelectronics, computer, and intelligent systems, from 2016 to 2018. He is currently an External Associate with the Faculty of Electrical Engineering and Computing, University of Zagreb. He is also a Software Developer with Ericsson Nikola Tesla d.d.

His research interests include affective computing, biomedical engineering, data mining, and signal processing.



ALAN JOVIC (M'08) received the B.Sc. and Ph.D. degrees in computer science from the Faculty of Electrical Engineering and Computing, University of Zagreb, Zagreb, Croatia, in 2006 and 2012, respectively. From 2006 to 2007, he was an Expert Associate with the Ruđer Bošković Institute, Zagreb. Since 2007, he has been with the Faculty of Electrical Engineering and Computing, University of Zagreb, where he is currently an Assistant Professor in computer science. His research interests include machine learning and data mining, biomedical engineering, and software engineering. His expertise lies in applications of artificial intelligence methods in biomedicine.

Dr. Jovic received the Vera Johanides Young Scientist Award from the Croatian Academy of Engineering in 2016.



MARIO CIFREK (M'97–SM'13) received the Dipl.Ing., M.Sc., and Ph.D. degrees in electrical engineering from the University of Zagreb, Croatia, in 1987, 1992, and 1997, respectively.

He is currently a Professor of electrical engineering with the Department of Electronic Systems and Information Processing, Faculty of Electrical Engineering and Computing, University of Zagreb. His research interests are focused on design of biomedical instrumentation and biomedical signal analysis for research and clinical applications.

Prof. Cifrek is a Senior Member of the IEEE Engineering in Medicine and Biology Society, the IEEE Instrumentation and Measurement Society, and the IEEE Signal Processing Society, the IEEE International Federation for Medical and Biological Engineering, the Croatian Biomedical Engineering and Medical Physics Society, and the Croatian Society for Communications, Computing, Electronics, Measurement, and Control. Since 2005, he has been a Collaborating Member of the Croatian Academy of Engineering.



GORAN KRSTACIC received the Ph.D. degree from the University of Zagreb, Croatia, in 2002.

He is currently an Associate Professor of cardiology with the School of Medicine, Josip Juraj Strossmayer University of Osijek, Croatia. He is a Specialist of internal medicine and cardiology and the CEO of the Institute for Cardiovascular Prevention and Rehabilitation, Zagreb. He is the coordinator of the E-Technology of the European Society of Cardiology. His research interests are non-invasive cardiology, heart rate variability, non-linear-dynamics, and chaos theory. He was the Chair of the Working Group on E-Cardiology.

He has authored or co-authored over 100 publications in international journals.

• • •